Journal of Applied Mechanics and Technical Physics, Vol. 46, No. 3, pp. 329–338, 2005

EFFECT OF BOUNDARY CONDITIONS ON TURBULENCE CHARACTERISTICS IN TWO-PHASE JET FLOWS WITH PHASE TRANSITIONS

Yu. V. Zuev

UDC 532.529

It is shown that there are no self-similarity and similarity of transverse fields of correlation moments of fluctuating parameters of phases in two-phase jets, in contrast to one-phase jets. The influence of the initial values of a number of parameters of a two-phase jet (gas temperature, volume concentration of droplets in the initial cross section, and radius of the initial cross section of the jet) on turbulence characteristics is analyzed on the basis of numerical simulations.

Key words: *turbulent jet, gas, droplets, turbulence characteristics, similarity, self-similarity.*

Introduction. Jet flows in nature and engineering devices are normally turbulent. The changes in all parameters of these flows, including the degree of their expansion, are determined by the turbulence characteristics of the jets. The study of fluctuating characteristics of jet flows is not only of academic interest but is also important for practice, e.g., for calculating the acoustic parameters of the jet. The microstructure of one-phase jet flows has been well studied. In particular, experiments revealed self-similarity and similarity of transverse fields of fluctuating velocities and their correlation moments in submerged jets.

The characteristics of turbulence of the phases can be found in papers dealing with experimental investigations of two-phase jets, e.g., in [1, 2], but the data obtained are not systematized and can be used only for testing mathematical models. No systematic theoretical investigation of turbulence characteristics in two-phase jets was performed either.

Calculated results for axisymmetric gas-droplet jets with phase transformations are given in the present work, which allows one to identify the influence of the initial values of some governing parameters of two-phase jets (boundary conditions) on turbulence characteristics.

Mathematical Model of a Two-Phase Turbulent Jet. The computations were based on the mathematical model described in [3], which consists of a system of averaged equations written in the boundary-layer approximation for each phase and the model of turbulence including expressions for correlation moments of fluctuating parameters of the phases. The discrete phase is described with the use of the particle-class concept. Particles of one class are characterized by identical values of size, velocity, temperature, and other parameters. In gas-phase equations, the parameters identical for all components (velocity and temperature) do not have any subscripts, and the parameters whose values are different for different components (density, specific heat, and volume concentration) are marked by the subscript k ($k = 1, 2, \ldots, K$); the parameters of droplets of class f in the equations are indicated by the subscript f ($f = 1, 2, \ldots, F$).

Each phase of the two-phase turbulent jet is described by the balance equations for mass, momentum, and energy. The equation of diffusion of the components is written for the gas phase, and the equation of changes in the droplet diameter due to coagulation, fragmentation, and phase transitions is derived for the droplet phase. These equations can be presented in the form

Moscow Aviation Institute (State Technical University), Moscow 125993; zuev@mail.ru. Translated from Prikladnaya Mekhanika i Tekhnicheskaya Fizika, Vol. 46, No. 3, pp. 29–40, May–June, 2005. Original article submitted March 9, 2004; revision submitted July 20, 2004.

$$A\,\frac{\partial U}{\partial x} + B\,\frac{\partial F}{\partial y} = -\frac{1}{y^{\beta}}\,\frac{\partial y^{\beta} G}{\partial y} + H, \tag{1}$$

where

$$A = \begin{bmatrix} 1 \\ 1 \\ u\sum_{k=1}^{K}(\rho_k\alpha_k) \\ \rho_f\alpha_f u_f \\ \rho_f\alpha_f u_f \\ u\sum_{k=1}^{K}(\rho_k\alpha_k) \\ \rho_f\alpha_f u_f \\ u\sum_{k=1}^{K}\rho_k\alpha_k \\ 1 \end{bmatrix}, \quad B = \begin{bmatrix} 1 \\ 1 \\ \sum_{k=1}^{K}(v\rho_k\alpha_k + \alpha_k\langle\rho_k' v'\rangle + \rho_k\langle\alpha_k' v'\rangle) \\ \rho_f(\alpha_f v_f + \langle\alpha_f' v_f'\rangle) \\ \rho_f(\alpha_f v_f + 2\langle\alpha_f' v_f'\rangle) \\ \sum_{k=1}^{K}(v\rho_k\alpha_k + \alpha_k\langle\rho_k' v'\rangle + \rho_k\langle\alpha_k' v'\rangle) \\ \rho_f(\alpha_f v_f + \langle\alpha_f' v_f'\rangle) \\ \sum_{k=1}^{K}(v\rho_k\alpha_k + \alpha_k\langle\rho_k' v'\rangle + \rho_k\langle\alpha_k' v'\rangle) \\ 0 \end{bmatrix}, \quad U = \begin{bmatrix} y^{\beta}u\sum_{k=1}^{K}\rho_k\alpha_k \\ y^{\beta}\rho_f\alpha_f u_f \\ u \\ u_f \\ v_f \\ c_pT \\ c_fT_f \\ \alpha_i \\ D_f^3 \end{bmatrix},$$

$$G = \begin{bmatrix} 0 \\ 0 \\ \sum_{k=1}^{K}(\rho_k\alpha_k)\langle u'v'\rangle \\ \rho_f\alpha_f\langle u_f'v_f'\rangle \\ \rho_f\alpha_f\langle v_f'^2\rangle \\ \sum_{k=1}^{K}(c_{pk}\rho_k\alpha_k)\langle T'v'\rangle \\ \rho_f\alpha_f c_f\langle T_f'v_f'\rangle \\ \langle\alpha_i'v'\rangle\sum_{k=1}^{K}(\rho_k\alpha_k) \\ 0 \end{bmatrix}, \quad F = \begin{bmatrix} y^{\beta}\sum_{k=1}^{K}(v\rho_k\alpha_k + \alpha_k\langle\rho_k' v'\rangle + \rho_k\langle\alpha_k' v'\rangle) \\ y^{\beta}\rho_f(\alpha_f v_f + \langle\alpha_f' v_f'\rangle) \\ u \\ u_f \\ v_f \\ c_pT \\ c_fT_f \\ \alpha_i \\ 0 \end{bmatrix},$$

$$H = \begin{bmatrix} -y^{\beta}\sum_{f=1}^{F}\vartheta_{f,p} \\ y^{\beta}(\vartheta_{f,p} + \vartheta_{f,c}) \\ -\frac{\partial P}{\partial x} - \sum_{f=1}^{F}F_{cfx} - \sum_{f=1}^{F}\vartheta_{f,p}(u_p - u) \\ F_{cfx} + \vartheta_{f,p}(u_p - u_f) + \sum_{j=1}^{F}\vartheta_{fj,c}(u_j - u_f) \\ -\frac{v_f}{y^{\beta}}\frac{\partial}{\partial y}y^{\beta}\rho_f\langle\alpha_f'v_f'\rangle + F_{cfy} + \vartheta_{f,p}(v_p - v_f) + \sum_{j=1}^{F}\vartheta_{fj,c}(v_j - v_f) \\ -\langle u'v'\rangle\sum_{k=1}^{K}\rho_k\alpha_k\frac{\partial u}{\partial y} + u\frac{\partial P}{\partial x} - \sum_{f=1}^{F}F_{cfx}(u_f - u) - \sum_{f=1}^{F}\vartheta_{f,p}E_{pk} - \sum_{f=1}^{F}Q_{\mathrm{conv}} \\ -\rho_f\alpha_f\langle u_f'v_f'\rangle\frac{\partial u_f}{\partial y} + \vartheta_{f,p}E_{pf} + \sum_{j=1}^{F}\vartheta_{fj,c}E_{fj} + Q_{\mathrm{conv}} \\ -\sum_{f=1}^{F}\vartheta_{f,p} \\ \frac{6}{\pi u_f}\sum_{j=1}^{f}K_{fj}e_{fj}F_{fj}\alpha_{fj} + \frac{D_f^3\vartheta_{f,p}}{\alpha_f\rho_f} \end{bmatrix}.$$

Equations (1) are supplemented by the equations of state of the phases

$$P = \rho_k R_k T, \qquad \rho_f = \text{const} \tag{2}$$

and by the equation relating the volume concentrations of the phases and components:

$$\sum_{k=1}^{K} \alpha_k + \sum_{f=1}^{F} \alpha_f = 1. \tag{3}$$

The specific drag force of droplets, the specific heat flux, and the terms responsible for phase transformations, coagulation, and fragmentation of droplets in Eqs. (1) are found by the formulas

$$\boldsymbol{F}_{cf} = 3\alpha_f C_{Df} \rho (\boldsymbol{W} - \boldsymbol{W}_f)|\boldsymbol{W} - \boldsymbol{W}_f|/(4D_f), \qquad C_{Df} = 0.32 + 4.4/\sqrt{\mathrm{Re}} + 24/\,\mathrm{Re},$$

$$Q_{\mathrm{conv}} = 6\alpha_{f,T}\alpha_f (T - T_f)/D_f, \qquad \alpha_{f,T} = D_f\,\mathrm{Nu}\,/\lambda, \qquad \mathrm{Nu} = 2 + 0.6\,\mathrm{Re}^{1/2}\,\mathrm{Pr}^{\,1/3},$$

$$\vartheta_{f,p} = 6\alpha_f D_k\,\mathrm{Sh}(\rho_{kn} - \rho_{ks})/D_f^2, \qquad E_{fj} = i_j - i_f + (u_j - u_f)^2/2,$$

$$E_{pk} = i_p - i_k(T) + (u_p - u)^2/2, \qquad E_{pf} = i_p - i_f(T_f) + (u_p - u_f)^2/2,$$

$$\vartheta_{f,c} = \frac{6\alpha_f}{\pi}\Big(\frac{1}{D_f^3}\sum_{j=1}^{f} K_{fj} e_{fj} \alpha_j \rho_j F_{fj} - \rho_f \sum_{j=f}^{F} \frac{\alpha_j}{D_j^3} K_{fj} e_{fj} F_{fj}\Big),$$

$$\sum_{j=1}^{F} \vartheta_{fj,c} E_{fj} = \frac{6\alpha_f}{\pi}\Big\{\frac{1}{D_f^3}\sum_{j=1}^{f} K_{fj} e_{fj} \alpha_j \rho_j E_{fj} + \rho_f \sum_{j=f}^{F} K_{fj} e_{fj}\,\frac{\alpha_j}{D_j^3}\,(1 - F_{fj}) E_{fj}\Big\},$$

$$\sum_{j=1}^{F} \vartheta_{fj,c} (u_j - u_f) = \frac{6\alpha_f}{\pi}\Big[\frac{1}{D_f^3}\sum_{j=1}^{f} K_{fj} e_{fj} \alpha_j \rho_j (u_j - u_f) + \rho_f \sum_{j=f}^{F} K_{fj} e_{fj}\,\frac{\alpha_j}{D_j^3}\,(1 - F_{fj})(u_j - u_f)\Big],$$

$$\sum_{j=1}^{F} \vartheta_{fj,c} (v_j - v_f) = \frac{6\alpha_f}{\pi}\Big[\frac{1}{D_f^3}\sum_{j=1}^{f} K_{fj} e_{fj} \alpha_j \rho_j (v_j - v_f) + \rho_f \sum_{j=f}^{F} K_{fj} e_{fj}\,\frac{\alpha_j}{D_j^3}\,(1 - F_{fj})(v_j - v_f)\Big].$$

In Eqs. (1)–(3) and other expressions given above for interphase interactions, $\boldsymbol{F}_{cf}$ and C_{Df} are the drag force and drag coefficient of droplets of class f, D_f and D_j are the diameters of droplets of classes f and j, respectively, D_k is the diffusivity of the vapor component of the gas phase, c_{pk} is the specific heat at constant pressure of the kth component of the gas phase, c_f is the specific heat of droplets of class f, K_{fj}, e_{fj}, and F_{fj} are the coagulation constant, capture coefficient, and escape coefficient of collisions of droplets of classes f and j [4], i is the specific enthalpy, i_p is the specific enthalpy of mass experiencing the phase transition, P is the pressure of the gas phase, R is the gas constant, Q_{conv} is the specific convective heat flux, T is the temperature, u and v are the projections of the velocity vector onto the x and y coordinate axes, u_p and v_p are the projections of the velocity vector of mass experiencing the phase transition onto the x and y coordinate axes, α is the volume concentration, $\alpha_{f,T}$ is the heat-transfer coefficient, λ is the thermal conductivity, ρ is the physical density, ρ_{kn} is the density of the vapor component of the gas phase, based on the partial pressure of this component, ρ_{ks} is the density of the vapor component of the gas phase, based on the pressure of saturated vapors of these components at the droplet temperature, $\vartheta_{f,p}$ is the mass converted from one aggregate state to another during a unit time in a unit volume of the medium owing to phase transitions (rate of phase transitions for a droplet of class f), $\vartheta_{f,c}$ is the change in mass of droplets of class f during a unit time in a unit volume of the medium owing to coagulation and fragmentation, $\vartheta_{fj,c}$ is the mass of droplets of class j in a unit volume of the medium, passing during a unit time to class f owing to coagulation and fragmentation, and Nu, Pr , Re, and Sh are the Nusselt, Prandtl, Reynolds, and Sherwood numbers. The fluctuating parameters of the phases are primed, the parameters of the components k and i of the gas phase are indicated by the subscripts k and i, and the parameters of droplets of classes f and j are marked by the subscripts f and j. The angular brackets denote space-time averaging. For axisymmetric and two-dimensional jets, $\beta = 1$ and $\beta = 0$, respectively.

Coagulation and fragmentation of droplets are calculated by the model developed by Shraiber and described in [4].

System (1)–(3) is solved under the following boundary conditions:

$$x = 0: \quad u = u(y), \quad \alpha_k = \alpha_k(y), \quad T = T(y), \quad u_f = u_f(y), \quad v_f = v_f(y),$$

$$\alpha_f = \alpha_f(y), \quad T_f = T_f(y), \quad k = 1, \ldots, K, \quad f = 1, \ldots, F;$$

$$y = \infty: \quad u = u_e, \quad \alpha_k = \alpha_{ke}, \quad T = T_e, \quad u_f = u_{fe}, \quad v_f = 0,$$

$$\alpha_f = \alpha_{fe}, \quad T_f = T_{fe}, \quad k = 1, \ldots, K, \quad f = 1, \ldots, F;$$

$$y = 0: \quad \frac{\partial u}{\partial y} = 0, \quad \frac{\partial \alpha_k}{\partial y} = 0, \quad \frac{\partial T}{\partial y} = 0, \quad k = 1, \ldots, K.$$

Parameters of the phases at the jet edge are indicated by the subscript e.

The system of averaged equations (1)–(3) is closed by expressions for correlation moments of fluctuating parameters of the phases, which are obtained with the use of Prandtl's model of turbulence extended to the case of two-phase flows [3]:

$$\langle u'v' \rangle = -K_u K_v l_0^2 \Big|\frac{\partial u}{\partial y}\Big| \frac{\partial u}{\partial y}, \quad \langle u'_f v'_f \rangle = -K_{uf} K_{vf} l_0^2 \Big|\frac{\partial u}{\partial y}\Big| \frac{\partial u}{\partial y}, \quad \langle v'^2_f \rangle = K^2_{vf} l_0^2 \Big(\frac{\partial u}{\partial y}\Big)^2,$$

$$\langle T'_f v'_f \rangle = -\frac{K_{vf} K_v}{\mathrm{Sc}_0} l_0^2 \Big|\frac{\partial u}{\partial y}\Big| \frac{\partial T_f}{\partial y}, \qquad \langle T'v' \rangle = -\frac{K_v^2}{\mathrm{Sc}_0} l_0^2 \Big|\frac{\partial u}{\partial y}\Big| \frac{\partial T}{\partial y}, \tag{4}$$

$$\langle \alpha'_k v' \rangle = -\frac{K_v^2}{\mathrm{Sc}_0} l_0^2 \Big|\frac{\partial u}{\partial y}\Big| \frac{\partial \alpha_k}{\partial y}, \quad \langle \alpha'_f v'_f \rangle = -\frac{K_{vf} K_v}{\mathrm{Sc}_0} l_0^2 \Big|\frac{\partial u}{\partial y}\Big| \frac{\partial \alpha_f}{\partial y}, \quad \langle \rho'_k v' \rangle = \frac{\rho_k}{T} \frac{K_v^2}{\mathrm{Sc}_0} l_0^2 \Big|\frac{\partial u}{\partial y}\Big| \frac{\partial T}{\partial y}.$$

In these expressions, l_0 is the Prandtl's mixing path in a single-phase jet, $K_u = u'/u'_0$, $K_v = v'/v'_0$, $K_{uf} = u'_f/u'_0$, $K_{vf} = v'_f/v'_0$, u', v', u'_f, and v'_f are the root-mean-square fluctuating velocities of the phases in the two-phase flow, u'_0 and v'_0 are the root-mean-square fluctuating velocities of the gas phase, the influence of droplets being ignored, and Sc_0 is the Schmidt number of the single-phase jet. The Schmidt number for an axisymmetric jet is assumed to be 0.8; the Prandtl's mixing path is calculated by the formula [5]

$$l_0^2 = B\Big[\Delta u_{\max}/(\partial u/\partial y)_{\max}\Big]^2,$$

where B is a constant (for axisymmetric jets, $B = 0.013$); $\Delta u_{\max}$ and $(\partial u/\partial y)_{\max}$ are the maximum values of the difference in streamwise velocities and the derivative of the streamwise velocity of the gas in the jet cross section considered.

The fluctuating velocities of the gas and droplets in expressions for correlation moments are calculated with the use of the turbulence model described in [6]. This model is a modification of Abramovich's model of turbulence for two phase flows [7]. Interaction of a gas volume (mole) of size l_0 with droplets located in the jet is considered in [6]. The sought phase velocities are determined by solving the system of equations including the equation of changes in momentum of the mole due to its interaction with droplets, the equation of motion of droplets in the mole, the equation of changes in the total energy of the mole due to its interaction with droplets, the equation of heat exchange between the droplets and the mole, the equations of state of the phases, and the equation relating the volume concentrations of the phases.

The partial differential equations are approximated by difference equations with the use of a second-order implicit six-point finite-difference scheme [8]. The nonlinear convective terms of the equations are written with the use of upwind and downwind differences. The system of difference equations is solved by the sweep method. The computation accuracy is monitored by the integral of excess energy of the phases, which should remain constant over the jet length. The deviation of this integral in various cross sections of the jet from its value in the initial cross section was within 4%.

The above-described mathematical model was compared in [9] with the models suggested in [1, 10–12]. In addition, the computations based on all these models were compared with the experiments of [1, 2], where the

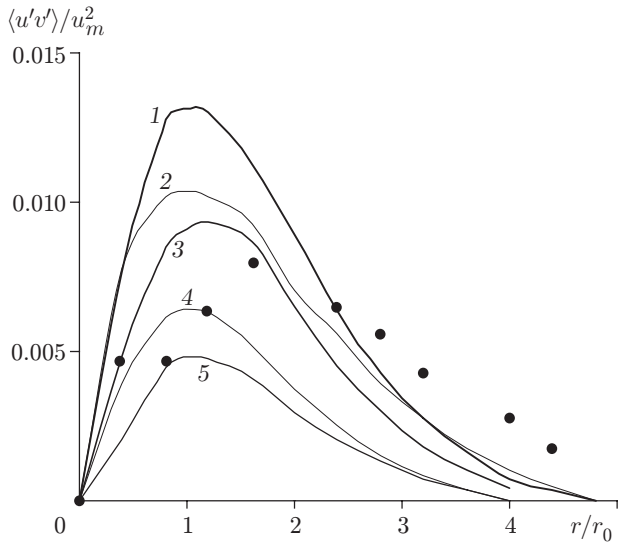

Fig. 1. Fields of the dimensionless correlation moment $\langle u'v'\rangle/\Delta u_m^2$ in the jet cross section $x/r_0 = 25$: data of [1] (curve 1), data of [12] (2), present work (3), data of [11] (4), and data of [10] (5); the points refer to the experimental data of [1].

TABLE 1

Computation variant	T_0, K	α_{f0}, 10^{-3}	r_0, mm
1	288	1,21	50
2	580	1.21	50
3	580	3.02	50
4	580	1.21	10

mean and fluctuating parameters of two-phase jets were measured. In terms of the mean parameters of the jet flow, all models were demonstrated to yield similar results, which were in good agreement with the experimental data. However, the above-described models give different turbulent characteristics of the phases. The degree of this difference can be evaluated from Fig. 1, which shows also the experimental data of [1], where the correlation moment of fluctuating velocities of the gas phase in an air jet with spherical glass particles about 100 μm in diameter with a mass flow-rate concentration of particles (ratio of the flow rates of the particles and the gas) equal to unity was measured. It is seen in Fig. 1 that the curve obtained by the model described in the present paper is located between the curves obtained with the use of other models and, with allowance for a large scatter of experimental points, is in satisfactory agreement with the experimental data.

It should be noted that the use of the models developed in [1, 10–12] involves difficulties associated with setting the boundary conditions for the turbulent kinetic energy and especially its dissipation rate. In addition, the models of [1, 10–12] contain up to 12 empirical constants, and some of them can be unknown functions of flow parameters. The turbulence model used in the present work ensures satisfactory agreement between numerical and experimental data with the use of only one empirical constant B in the expression for the mixing path, which is assumed to be equal to the value of this constant for single-phase jets. This model of turbulence makes it possible to calculate two-phase jets by setting the boundary conditions for averaged parameters of the phases only.

Effect of the Boundary Conditions on Characteristics of Turbulence in Jets with Phase Transformations. Computation results for axisymmetric gas-droplet jets with phase transformations presented below reveal the influence of the initial values of some governing parameters of two-phase jets on turbulence characteristics. The parameters varied in the computations were the gas temperature, the volume concentration of droplets in the initial cross section of the jet, and the radius of the initial cross section of the jet (radius of the nozzle from which the jet escapes). The values of these parameters are listed in Table 1. The following values were used in all computation variants for the remaining parameters: ambient gas pressure $P = 0.1$ MPa; droplet diameter $D_f = 50$ μm;

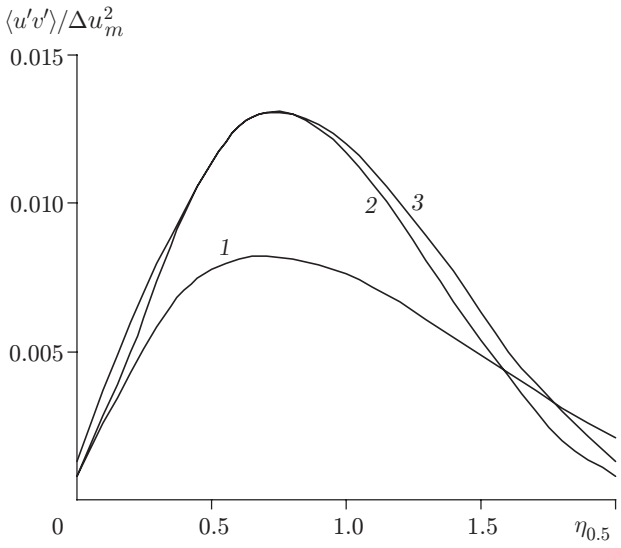

Fig. 2

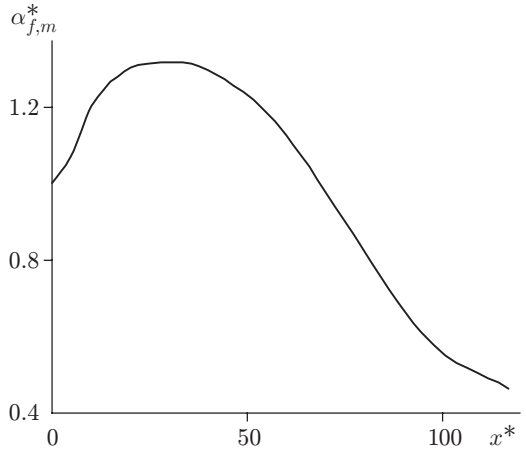

Fig. 3

Fig. 2. Dimensionless correlation moment in different cross sections of a two-phase jet (computation variant No. 2): $x^* = x/r_0 = 100$ (curve 1), 200 (2), and 500 (3).

Fig. 3. Volume concentration of droplets along the centerline of a two-phase jet (computation variant No. 2).

parameters of the gas and droplets at the nozzle exit: gas velocity $u_0 = 50$ m/sec, droplet velocity $u_{f0} = 50$ m/sec, and droplet temperature $T_{f0} = 288$ K; parameters of the gas and droplets in the ambient medium: gas temperature $T_e = 288$ K, droplet temperature $T_{fe} = 288$ K, gas velocity $u_e = 0.01$ m/sec, droplet velocity $u_{fe} = 0.01$ m/sec, volume concentration of droplets $\alpha_{fe} = 10^{-8}$, and volume concentration of water vapors $\alpha_{ke} = 0.01193$. Air jets containing water droplets and exhausting into the air medium were considered. The fields of all parameters of these jets at the nozzle exit were uniform.

Figure 2 shows the dimensionless correlation moment of fluctuating velocities of the gas phase as a function of the dimensionless coordinate $\eta_{0.5} = r/r_{0.5u}$ ($\Delta u_m = u_m - u_e$, where u_m and u_e are the gas velocities at the jet centerline and in the ambient space, respectively; r is the current value of the jet radius, and $r_{0.5u}$ is the jet radius corresponding to $\Delta u/2$), which was obtained in the computation variant No. 2 for five cross sections of a nonisothermal two-phase jet with phase transitions (the curves for the cross sections $x^* = 300$ and 400, which are not shown in the figure, are located between curves 2 and 3). In this computation variant, the dimensionless transverse fields of the correlation moment in the jet almost coincide with each other, beginning from the distance $x^* = 200$. Hence, the jet considered contains a region where the flow is self-similar in terms of the parameter $\langle u'v'\rangle/\Delta u_m^2$ (self-similarity is understood as the shape of the dimensionless field of a certain flow parameter being independent of the streamwise coordinate). In a two-phase jet with phase transformations, because of suction of air from the ambient space and evaporation of liquid droplets, the concentration of droplets drastically decreases, beginning from the cross section $x^* \approx 40$ (evolution of the dimensionless volume concentration of droplets along the jet centerline is shown in Fig. 3). In the cross section $x^* = 200$, the jet, which was a two-phase medium at a smaller distance from the nozzle, becomes a single-phase multispecies jet. At the jet part with a sufficiently high concentration of droplets (in our case, at $x^* < 200$), the presence of these droplets leads to suppression of turbulence of the gas phase, which is reflected in the magnitude of the correlation moment $\langle u'v'\rangle/\Delta u_m^2$ (its value is lower than that in a single-phase jet). Beginning from a certain cross section, the jet flow becomes a single-phase one, and this region of the jet displays self-similarity of transverse fields of the correlation moment $\langle u'v'\rangle/\Delta u_m^2$, which coincide with the corresponding parameter of a single-phase jet. The same results were obtained in the computation variant No. 3, which differs from the computation variant No. 2 by a higher concentration of droplets in the initial cross section of the jet (by a factor of 2.5). In this variant, the transverse fields of the correlation moment $\langle u'v'\rangle/\Delta u_m^2$ become self-similar, beginning from the cross section $x^* = 300$.

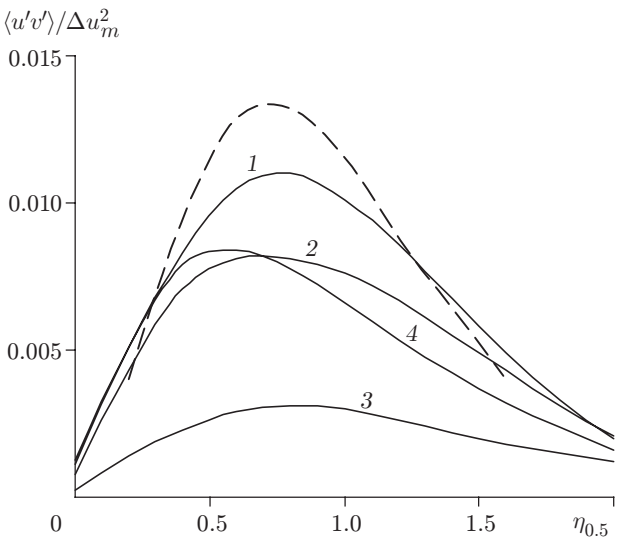

Fig. 4. Dimensionless correlation moment of fluctuating velocities of the gas phase in the corresponding cross sections x^*_{100} of two-phase jets with different boundary conditions: the numbers at the curves correspond to the numbers of the computation variants; the dashed curve shows the field of the dimensionless correlation moment in the gas jet.

The influence of the boundary conditions on the transverse fields of the correlation moment $\langle u'v'\rangle/\Delta u_m^2$ can be traced by analyzing the data in Fig. 4, which shows the dependences $\langle u'v'\rangle/\Delta u_m^2 = f(\eta_{0.5})$ for four computation variants for two-phase jets (see Table 1) in the cross section $x^* = 100$ (in what follows, this cross section is denoted as x^*_{100} for brevity). It follows from this figure that different computation variants yield different transverse fields of the dimensionless correlation moment in those regions of two-phase jets where the influence of droplets on turbulent characteristics of the phases in these jets is manifested. This means that there is no similarity of the transverse fields of the correlation moment $\langle u'v'\rangle/\Delta u_m^2$ in these regions of two-phase jets (similarity of the transverse fields is understood as the coincidence of dimensionless fields of identical parameters in the corresponding cross sections of the jets).

According to Eq. (4), the value of the correlation moment $\langle u'v'\rangle/\Delta u_m^2$ in two-phase jets is affected by the transverse gradient of the mean velocity of the gas and the gas-phase fluctuating velocities depending on the droplet concentration and diameter.

All computation variants predict similar transverse fields of the gas velocity in the jet cross sections x^*_{100}; hence, the transverse gradient of the gas velocity can be ignored in comparing these variants.

Varaksin [13] suggested that the Stokes number in the averaged, large-scale, and small-scale oscillatory motion should be used to determine the character of gas–particle interaction. The flow regime in which the particles act as a passive admixture, i.e., are completely entrained by turbulent vortices, can be determined by only one Stokes number $\mathrm{Stk} = \rho_f D_f^2 u/(36\mu r_b)$ based on the local averaged parameters of the jet: density of the droplet substance ρ_f, droplet diameter D_f, viscosity of the gas phase μ, and radius of the jet boundary r_b. Kostyuk et al. [9] showed that the particles can be regarded as a passive admixture for $\mathrm{Stk} \leqslant 0.144$. In this case, the particle size does not affect turbulence characteristics; the latter depend on the particle concentration only. The value of the Stokes number above which the particle size has no effect on turbulence characteristics was called the critical value (Stk_*) [9].

Figure 5 shows the Stokes number in the cross sections x^*_{100} of two-phase jets in different computation variants. In all variants, the Stokes number has the maximum value at the centerline and decreases with distance from the centerline because of the decrease in the gas-phase velocity and the size of droplets due to their evaporation. In the computation variant Nos. 1 and 2, the values of the Stokes number at the jet centerline are close to Stk_* or lower than Stk_* in a wide range of variation of the jet radius. In these computation variants, therefore, the values of $\langle u'v'\rangle/\Delta u_m^2$ in the jet cross sections x^*_{100} should be independent of the droplet diameter but should be related to the volume concentration of droplets in these cross sections. Indeed, a comparison of the dependences

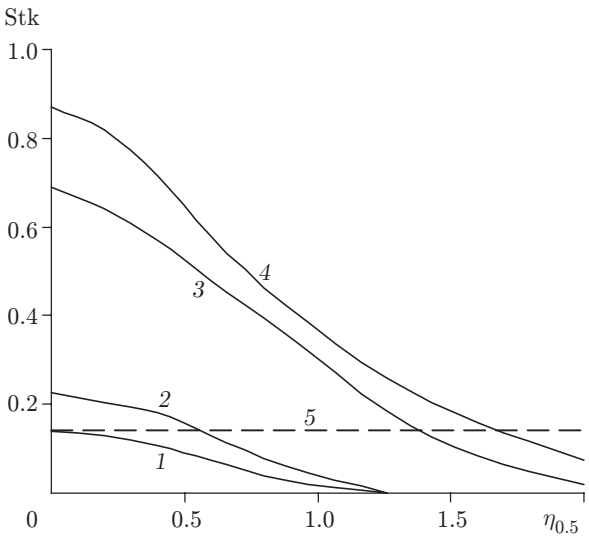

Fig. 5. Stokes number in the corresponding cross sections x^*_{100} of two-phase jets with different boundary conditions: the numbers at the curves (1–4) correspond to the numbers of the computation variants; the straight line 5 shows the critical Stokes number.

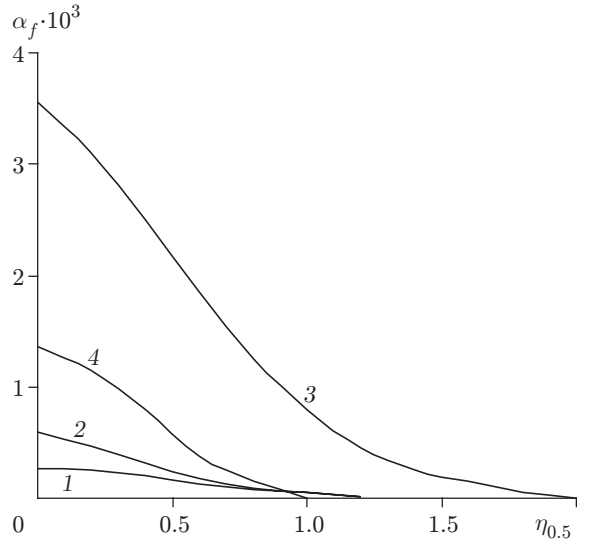

Fig. 6. Transverse fields of the volume concentration of droplets in the cross sections x^*_{100} of two-phase jets with different boundary conditions: the numbers at the curves correspond to the numbers of the computation variants.

$\langle u'v' \rangle / \Delta u_m^2 = f(\eta_{0.5})$ plotted in Fig. 4 with the dependences $\alpha_f = f(\eta_{0.5})$ in Fig. 6 shows that they are correlated: the higher the volume concentration of droplets in the corresponding cross sections of the jet, the lower the value of the considered correlation moment in these cross sections.

It follows from Fig 5 that the magnitude of the correlation moment of fluctuating velocities of the gas phase in the computation variant No. 3 ($\mathrm{Stk} > \mathrm{Stk}_*$) should be affected by both the volume concentration and the size of droplets (more exactly, the dimensionless size of droplets $D_f^* = D_f / r_b$). An increase in the droplet concentration should decrease the fluctuating velocities of the gas, and the increase in the dimensionless droplet diameter should increase this parameter and, hence, the correlation moments. In accordance with the computations performed, the dimensionless size of droplets at the jet centerline in the cross section x^*_{100} is 10^{-4} in variant No. 1, $1.3 \cdot 10^{-4}$ in variant No. 2, $2 \cdot 10^{-4}$ in variant No. 3, and $5.6 \cdot 10^{-4}$ in variant No. 4. The dimensionless droplet size decreases

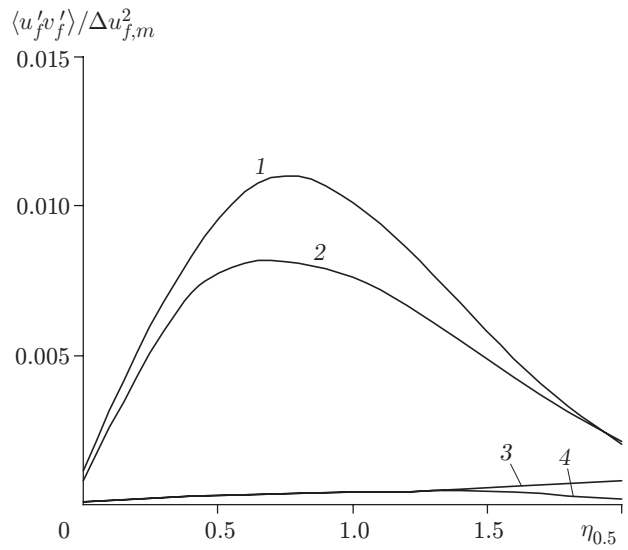

Fig. 7. Dimensionless correlation moment of fluctuating velocities of the discrete phase in the cross sections x^*_{100} of two-phase jets with different boundary conditions: the numbers at the curves correspond to the numbers of the computation variants.

in the radial direction with distance from the jet centerline. In the computation variant No. 3, the dimensionless droplet size in the jet cross section x^*_{100} exceeds the corresponding value in the computation variant Nos. 1 and 2, but the droplet concentration in the jet cross section is substantially higher (see Fig. 6). The effect of the volume concentration of droplets on the correlation moment $\langle u'v' \rangle / \Delta u^2_m$ in the computation variant No. 3 is stronger than the effect of the droplet size; hence, the value of the correlation moment of fluctuating velocities of the gas phase in this computation variant is lower than that in the computation variant Nos. 1 and 2.

The distribution of the dimensionless correlation moment of fluctuating velocities of the gas phase over the jet cross section in the computation variant No. 4 (curve 4 in Fig. 4) corresponding to a smaller radius of the initial jet cross section is close to that in the computation variant No. 2 (curve 2 in Fig. 4). This occurs for the following reason. With initial cross section of the jet decreasing in the computation variant No. 4, the dimensionless droplet diameter in the jet cross section x^*_{100} increases by more than a factor of 4, as compared to the computation variant No. 2, which should have increased the intensity of turbulence of the gas phase. However, as the dimensionless droplet diameter increases, the coefficient of turbulent diffusion of droplets decreases; as a result, the volume concentration of droplets in the jet cross section considered increases (see Fig. 6), which should lead to a decrease in the correlation moment of fluctuating velocities of the gas phase. These two effects resulting from the increase in the dimensionless droplet diameter (in the considered range of its variation) compensated for each other; as a result, the computed transverse field of the dimensionless correlation moment $\langle u'v' \rangle / \Delta u^2_m$ depends weakly on the size of the initial cross section of the jet.

For all computation variants, the transverse fields of the correlation moment $\langle u'v' \rangle / \Delta u^2_m$ in the jet cross section $x^* = 500$ coincide with each other and with the transverse field of this correlation moment for a single-phase jet. Hence, independent of the boundary conditions, two-phase jets display similarity of the transverse fields of the correlation moment $\langle u'v' \rangle / \Delta u^2_m$ in jet regions far from the nozzle, where the volume concentration of droplets becomes so small that the droplets do not affect the turbulent characteristics of the phases in these jets.

Figure 7 shows the transverse fields of the correlation moment $\langle u'_f v'_f \rangle / \Delta u^2_{f,m}$ ($\Delta u_{f,m}$ is the difference in velocities of droplets at the jet centerline and at its boundary) in the cross sections x^*_{100} of jets with different boundary conditions. The numbers at the curves correspond to the numbers of the computation variants. Curves 1 and 2 in this figure coincide with curves 1 and 2 in Fig. 4, i.e., in the computation variant Nos. 1 and 2, the correlation moments $\langle u'v' \rangle / \Delta u^2_m$ and $\langle u'_f v'_f \rangle / \Delta u^2_{f,m}$ in the jet cross section x^*_{100} coincide, which can occur only in the case of a moderate dimensionless size of droplets ($\mathrm{Stk} < \mathrm{Stk}_*$; see Fig. 5) whose relaxation time is smaller than or close to the integral time scale of turbulence of the gas phase.

Curves 3 and 4 in Fig. 7 are located much lower than curves 1 and 2, i.e., the correlation moment $\langle u'_f v'_f \rangle / \Delta u^2_{f,m}$ in the computation variant Nos. 3 and 4 is substantially lower than that in the computation variant Nos. 1 and 2. The reason is that the droplets in the jet cross section x^*_{100} in the computation variant Nos. 3 and 4, as compared to the computation variant Nos. 1 and 2 have, first, a greater dimensional diameter (with $\mathrm{Stk} > \mathrm{Stk}_*$; see Fig. 5) and, therefore, are less readily involved into oscillatory motion, and second, a higher concentration (see Fig. 6), which ensures stronger suppression of gas turbulence by droplets and, as a consequence, decreases the fluctuating velocities of droplets. Since $\mathrm{Stk} > \mathrm{Stk}_*$ in the computation variant Nos. 3 and 4, the transverse fields of the correlation moment $\langle u'v' \rangle / \Delta u^2_m$ (see Fig. 4) do not coincide with the transverse fields of the correlation moment $\langle u'_f v'_f \rangle / \Delta u^2_{f,m}$ (see Fig. 7); a greater difference in the values of these correlation moments is observed in variant No. 4. The result obtained is explained by a significant difference in fluctuating velocities of the gas and droplets in the computation variant No. 4 in the cross section x^*_{100}, which is caused by the above-noted influence of the dimensionless diameter and concentration of droplets on turbulent characteristics of the phases (interaction of the phases in oscillatory motion becomes weaker with increasing dimensionless diameter and decreasing droplet concentration).

Conclusions. In the regions of two-phase jets with phase transitions, where the droplet concentration is sufficient to affect the parameters of these jets, there is no similarity or self-similarity of transverse fields of all characteristics of turbulence in the gas and disperse phase. In the regions of two-phase jets far from the nozzle, where the droplet concentration becomes very low because of turbulent diffusion of droplets and mainly because of their evaporation, the transverse fields of turbulence characteristics of the gas phase become similar and self-similar, as in single-phase jets. The correlation moments of fluctuating velocities of small droplets whose local Stokes numbers are lower than the critical value are the same as the corresponding characteristics in the gas phase.

REFERENCES

1. A. A. Mostafa, H. C. Mongia, V. G. McDonell, and G. S. Samuelsen, "On the evolution of particle-laden jet flows: A theoretical and experimental study," *AIAA J.*, 2181–2197 (1987).
2. D. Modarress, H. Tan, and S. Elghobashi, "Two-component LDA measurement in a two-phase turbulent jet," *AIAA J.*, **22**, No. 5, 624–630 (1984).
3. Yu. V. Zuev and I. A. Lepeshinskii, "Two-phase multispecies turbulent jet with phase transitions," *Izv. Ross. Akad. Nauk, Mekh. Zhidk. Gaza*, No. 5, 120–138 (1995).
4. L. E. Sternin, *Fundamentals of Gas Dynamics of Two-Phase Flows in Nozzles* [in Russian], Mashinostroenie, Moscow (1974).
5. G. N. Abramovich, S. Yu. Krasheninnikov, and A. N. Sekundov, *Turbulent Flows under the Action of Bulk Forces and Non-Self-Similarity* [in Russian], Mashinostroenie, Moscow (1975).
6. Yu. V. Zuev, I. A. Lepeshinskii, V. A. Sovetov, and V. A. Chabanov, "Calculation of fluctuating parameters of the phases in a multiphase multispecies nonisothermal nonequilibrium jet," *Inzh.-Fiz. Zh.*, **49**, No. 3, 503–504 (1985).
7. G. N. Abramovich (ed.), *Theory of Turbulent Jets* [in Russian], Nauka, Moscow (1984).
8. V. M. Paskonov, V. I. Polezhaev, and L. A. Chudov, *Numerical Simulation of Heat- and Mass-Transfer Processes* [in Russian], Nauka, Moscow (1984).
9. V. V. Kostyuk, Yu. V. Zuev, I. A. Lepeshinskii, et al., "Investigation of interphase interaction in multiphase turbulent jets," *Mat. Model.*, **11**, No. 4, 59–69 (1999).
10. A. A. Shraiber, L. B. Gavin, V. A. Naumov, and V. P. Yatsenko, *Turbulent Gas-Suspension Flows* [in Russian], Naukova Dumka, Kiev (1987).
11. S. Elghobashi, T. Abou-Arab, M. Rizk, and A. Mostafa, "Prediction of the particle-laden jet with a two-equation turbulence model," *Int. J. Multiphase Flow*, **10**, No. 6, 697–710 (1984).
12. E. P. Volkov, L. I. Zaichik, and V. A. Pershukov, *Modeling of Combustion of Solid Fuels* [in Russian], Nauka, Moscow (1994).
13. A. Yu. Varaksin, *Turbulent Gas Flows with Solid Particles* [in Russian], Fizmatlit, Moscow (2003).